Article

Journal of
Nanoscience and Nanotechnology
Vol. 18, 1–9, 2018
www.aspbs.com/jnn

Measuring the Acoustic Release of a Chemotherapeutic Agent from Folate-Targeted Polymeric Micelles

Ayah Abusara, Mamoun Abdel-Hafez, and Ghaleb Husseini*

College of Engineering, American University of Sharjah, Sharjah, UAE

In this paper, we compare the use of Bayesian filters for the estimation of release and re-encapsulation rates of a chemotherapeutic agent (namely Doxorubicin) from nanocarriers in an acoustically activated drug release system. The study is implemented using an advanced kinetic model that takes into account cavitation events causing the antineoplastic agent's release from polymeric micelles upon exposure to ultrasound. This model is an improvement over the previous representations of acoustic release that used simple zero-, first- and second-order release and re-encapsulation kinetics to study acoustically triggered drug release from polymeric micelles. The new model incorporates drug release and micellar reassembly events caused by cavitation allowing for the controlled release of chemotherapeutics specially and temporally. Different Bayesian estimators are tested for this purpose including Kalman filters (KF), Extended Kalman filters (EKF), Particle filters (PF), and multi-model KF and EKF. Simulated and experimental results are used to verify the performance of the above-mentioned estimators. The proposed methods demonstrate the utility and high-accuracy of using estimation methods in modeling this drug delivery technique. The results show that, in both cases (linear and non-linear dynamics), the modeling errors are expensive but can be minimized using a multi-model approach. In addition, particle filters are more flexible filters that perform reasonably well compared to the other two filters. The study improved the accuracy of the kinetic models used to capture acoustically activated drug release from polymeric micelles, which may in turn help in designing hardware and software capable of precisely controlling the delivered amount of chemotherapeutics to cancerous tissue.

Keywords: Micelles, Drug Encapsulation, Ultrasound, Kalman Filter, Extended Kalman Filter, Particle Filter.

1. INTRODUCTION

Chemotherapeutic agents have adverse side effects due to their cytotoxic effects on healthy tissue. These side effects include but are not limited to nausea, leukopenia, alopecia, a reaction at the site of injection and cardiotoxicity.[1] Hence the need arises for scientist and engineers to synthesize drug delivery systems capable of preferentially targeting diseased cells. There are three broad types of targeting in the area of drug delivery: passive, ligand (active) and triggered. These three targeting techniques are utilized to design a 'guided missile' or a "magic bullet" for cancer treatment. "Passive" targeting refers to the increased accumulation of the carrier inside the leaky vasculature of tumors due to the enhanced permeability and retention effect. "Active-" or "ligand-" targeting is used to describe ligand-receptor interactions and allows for the increased accumulation of the carrier via endocytosis. Finally, triggered targeting involves the release of the chemotherapeutic in response to external or internal stimuli. External means include temperature, magnetic fields, light, ultrasound, and electromagnetic waves, while internal stimuli include pH, enzymes, electron affinity and reduction potentials.

The drug delivery system under investigation involves the sequestration of chemotherapeutic agents inside the core of polymeric micelles and then the use of ultrasound to release the nanocarriers' contents.[1,2] Those nanocarriers (10–100 nm) are micellar in structure and can serve as a possible drug carrier to hydrophobic agents used in chemotherapy. Micelles are composed of amphiphilic di- and tri-block copolymers.[3,4] The amphiphilic copolymers are composed of hydrophobic heads and hydrophilic tails that allow the encapsulation of hydrophobic agents. An added advantage of the hydrophilic polymeric tails is their

*Author to whom correspondence should be addressed.

poly-ethylene glycol (PEG) structure which renders them unrecognized by the reticulo-endothelial system (RES) and hence allows for a long circulation time in the blood.[5] The nanovehicles used in this study are composed of Pluronic® P105. Pluronic® P105 micelles are formed when the triblock copolymer (composed of polyethylene oxide-polypropylene oxide-polyethylene oxide) is dissolved in water to a concentration above its critical micelle concentration (CMC).[6, 7] During the micellization process, the hydrophobic polypropylene blocks form the core region of the micelle and the hydrophilic polyethylene glycol blocks act as the interface between the core spherical region and the external aqueous medium. Once Pluronic P105 micelles are formed, the hydrophobic chemotherapeutic agents accumulate inside its core. The premise of this drug delivery system is that the drug is encapsulated and is allowed to circulate in the body until it reaches the cancerous site. Once there, a trigger mechanism is needed to release the chemotherapeutic agents to the desired tissue, and ultrasound appears to ideally fulfil this role.[8, 9]

Ultrasound waves are high-frequency sound waves, with frequencies typically greater than 20 kHz. Ultrasound is used as an imaging technique to produce images of body organs. These images are created by converting the echoes of the sound waves into sonograms. These acoustic waves can penetrate deep into the body without a surgical incision. In addition to its non-invasive nature, ultrasound has many advantages that render it useful as a trigger mechanism in drug delivery, including: the fact that ultrasound waves can be controlled and focused on the tumor site, the well-documented synergistic effect that exists between the activity of drugs and ultrasound,[10, 11] the ability of ultrasound to enhance the transport of drugs through tissues and other membranes,[12] and that ultrasound-induced hyperthermia has the ability to eradicate cancerous cells.[13, 14] Ultrasound-based drug release may occur due to two phenomena: sonoporation, and collapse cavitation. In sonoporation, ultrasound causes temporal permeability in the membrane of cells allowing for subsequent drug uptake. In the collapse cavitation stage, ultrasound intensity causes the collapse of microbubbles which causes the formation of ultrasound shock waves. When these shock waves reach the micelles, they shear the micellar structure open, releasing the encapsulated drug in the process.[15–17]

In addition to passive- and triggered-targeting, ligand-/active-targeting can be achieved via the conjugation of targeting moieties to the surface of the carriers. One of the most important ligands used in drug delivery is the folate/folic acid moiety because its receptors are overexpressed on the surface of many cancer cells (including breast and ovarian cancers).

We have reported earlier the release of Doxorubicin and Ruboxyl from Pluronic® P105 micelles and have analyzed its release kinetics using mechanistic-deterministic models[18, 19] and stochastic models.[20–22] In a previous paper, the drug release was mathematically modeled and the estimation of the drug release and encapsulation was captured using Kalman filters.[23] The estimation performance was also enhanced using an adaptive Kalman filter that is more resistant to modeling errors. In this work, we take it a step further with a more realistic drug release model and use several Bayesian filters. Both Kalman and particle filters belong to the class of Bayesian estimators. Kalman filters are optimal estimators when used in linear and Gaussian models,[24] however, they work only under these constraints. For non-linear models, extended Kalman filters are widely used. EKFs use the standard Kalman filter formulation for non-linear estimates by linearizing about the estimate at each step. EKFs have the capability of producing accurate results when used in the solution of many problems, yet diverge for others because the optimality of EKF depends on the degree of the non-linearity of the model.[25] Therefore, we investigate the more general Bayesian estimators known as particle filters. A particle filter is a sequential Monte Carlo-based mathematical tool also known as a Bootstrap Filter. Particle filters are powerful tools when used for nonlinear and non-Gaussian distributed systems. Although particle filters are counted as sub-optimal filters when compared to other Bayesian filters, they approach optimality as the number of particles is increased.[25] The performance of the Kalman filter and the adaptive Kalman filter proposed in a previous publication[23] will be compared against the performance of particle filters. The drug release model used in this work will also be extended to include non-linearities that account for the reconstruction of micelles addressed earlier.[26] For that model, EKF, adaptive EKF and particle filters will be used to estimate the drug encapsulation percent. Our objective in this paper is to study and analyze those Bayesian estimators when applied to our drug delivery system. More specifically, the study aims to improve the accuracy of the kinetic models used to capture acoustically activated drug release from polymeric micelles, which may in turn help in designing hardware and software capable of precisely controlling the delivered amounts of chemotherapeutics to cancerous tissue.

2. MATERIALS AND METHODS

2.1. Drug Encapsulation in Pluronic Micelles

Stock solutions of Pluronic® P105 (a gift from BASF, Mount Olive, NJ) were prepared by dissolving the polymer in a PBS (phosphate buffered saline) solution to a final concentration of 10% wt. Doxorubicin-Dox (Pharmacia and Upjohn Company Kalamazoo MI), in dosage form (1:5, Dox: lactose), was dissolved in the P105 solutions at room temperature to produce a final Dox concentration of 4.5 μg/ml in 5% wt. Pluronic®. The drug was encapsulated inside both non-targeted and folate-targeted Pluronic® P105 micelles.[11] As a control, the same drug concentration was also prepared in PBS.

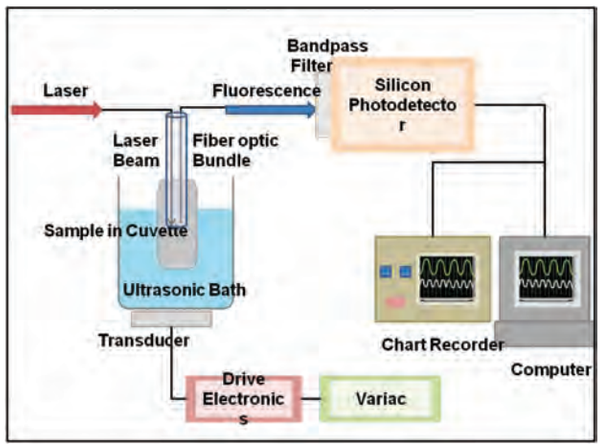

Figure 1. Fluorescence detection in an ultrasound exposure chamber.

2.2. Measuring the Acoustic Release from Micelles

To quantify drug release, a custom-made chamber was built to measure the change in fluorescence and hence the Dox release in the presence and absence of ultrasound.[27] The chamber is illustrated in Figure 1. Micelles encapsulating Dox were pipetted in an acoustically transparent tube in a sonicating bath filled with degased water (Sonicor SC-50, Copiaque, NY) with the sample placed directly above the transducer. The signal generated by the transducer can be described as a 70-kHz wave amplitude-modulated sinusoidally at about 0.12 kHz. A fiber optic probe was inserted inside the sample-containing chamber to direct the laser excitation beam into the sample and collect the emitted fluorescence from the Dox molecules. A Bruel and Kjaer hydrophone (# 8103, Decatur, GA) was used to measure the acoustic power density delivered. The release was examined at several power densities corresponding to mechanical indices in the stable and transient cavitation regions. Calculations showed that 99% of the collected fluorescence originated within 3 mm of the tip of the fiber optic bundle. The % Dox release was calculated from the fluorescence measurements using the equation below and assuming a linear behavior:

$$\%\text{release} = \frac{I_{\text{P105}} - I_{\text{US}}}{I_{\text{P105}} - I_{\text{PBS}}} \times 100\%$$

where I_{US} is the fluorescence intensity upon exposure to ultrasound, I_{PBS} is the fluorescence intensity in a solution of Dox in PBS, and I_{P105} is the intensity recorded when the drug is encapsulated in Pluronic® P105 (which corresponds to 0% release or 100% encapsulation).

3. MECHANISTIC DYNAMIC MODEL

The first model used in this paper is based on the mathematical formulation proposed earlier,[18] which suggests that the drug is acoustically released from micelles at a constant rate. When ultrasound is turned off the re-encapsulation rate is first-order with respect to the released drug concentration.[23] The model is represented by the following equation:

$$\frac{dE(t)}{dt} = -k_{\text{r}} + k_{\text{e}}(T - E(t))$$

where $E(t)$ is the encapsulated drug amount at time t and $dE(t)/dt$ is the rate of change of drug encapsulation. T is the drug concentration in the solution (inside and outside micelles), k_{r} is a zero-order release rate constant, and k_{e} is a first order re-encapsulation rate constant.[23] The above is discretized at a sampling time $\Delta t = 0.2$ sec.[23] The system model is then given by:

$$E(k) = e - k_{\text{e}}\Delta t E(k-1) + Bd + w(k-1)$$

where $Bd = (e - k_{\text{e}}\Delta t - 1)(k_{\text{r}} - 1)$ and $w(k)$ is the system noise modeled as zero-mean Gaussian white noise with covariance R. The measurement model equation is shown below:

$$y(k) = E(k) + v(k)$$

where $v(k)$ is the measurement noise modeled as zero-mean Gaussian white noise with covariance Q.

The second model used in this paper is an extension to the dynamics of the drug encapsulation in $dE(t)/dt = -k_{\text{r}} + k_{\text{e}}(T - E(t))$ to involve a competing mechanism to the drug release, which is the drug reassembly. The model is based on transient cavitation events causing shock waves to shear open these nanovehicles. Upon the termination of sonication, the polymeric chains will reassemble into the micellar structure again. Doxorubicin will reaccumulate inside the hydrophobic poly-propylene core of the micelles resulting in drug "re-encapsulation." The formulation of the drug release process and its counteract can be derived from the micelles destruction and reassembly formulas. The latter is apparent in the rate of change of the number of micelles:

$$\frac{dM_j}{dt} = \left(\frac{dM_j}{dt}\right)_{\text{destruction}} + \left(\frac{dM_j}{dt}\right)_{\text{assembly}}$$

Using our previous report,[26] the above expression can be expressed as:

$$\frac{dM_j}{dt} = [-\alpha \bar{D}_j M_j e^{-k_n t}] + \left[\left(\frac{\beta}{\bar{D}_j^3}\right)\left(1 - n\frac{\sum_{j=1}^{n} M_j D_j^3}{\sum_{j=1}^{n} D_j^3}\right)\right]$$

The first part of the above equation is attributed to the destruction of micelles where α is a non-zero constant and $\bar{D}_j$ is the size of the micelle. The exponential expression, however, represents the cavitating nuclei which decreases exponentially over time with a non-zero constant factor equal to k_n. The second part of the formula, on the other hand, represents the reassembly of the destructed micelles, where β is a non-zero constant and the inverse of the size of the micelle cubed D_j^3 are multiplied by an expression for the concentration volume.[26]

In the same manner, the drug encapsulation rate is formulated as:

$$\frac{dE_j}{dt} = \left(\frac{dE_j}{dt}\right)_{\text{release}} + \left(\frac{dE_j}{dt}\right)_{\text{encapsulation}}$$

where,

$$\frac{dE_j}{dt} = [-\alpha \bar{D}_j M_j e^{-k_n t} E_j] + \left[\lambda F M_j \frac{\bar{D}_j^3}{\bar{D}_j \sum_{j=1}^{n} \bar{D}_j^3}\right]$$

The relation between drug release and the destruction of micelles is evident in the above formula. The same applies to the drug encapsulation and micellar reassembly, where F represents the free drug and λ is a non-zero constant. Obtaining the system dynamic equation from the equation above is not straightforward. Hence, MATLAB® fitting tools were deployed for this purpose. Simulation results showed that the model that best fits the data generated by the above differential equations is a quadratic model with the following structure:

$$E(k) = \alpha(E(k-1))^2 + \beta E(k-1) + \gamma + w(k-1)$$

where β and γ are non-zero constants. Since, the encapsulation rate can be measured directly, the measurement equation remains as:

$$y(k) = E(k) + v(k)$$

4. THE PROPOSED ESTIMATION APPROACHES

4.1. Kalman Filter

Kalman filters are Bayesian filters that are used to predict the state of a system given online measurements of that state. The state estimation is achieved by investigating the probability $p(E \mid Y^k)$ of the state, in our case the encapsulation rate E, which results in the online observations, where $Y^k = [y(0), y(1), \ldots, y(k)]$ are the state observations (measurements) up to time k. Kalman filters provide the MMSE estimate that maximizes $\operatorname{argmax}_E\, p(E \mid Y^k)$ which happens to be the mean $\overline{(E \mid Y^k)}$. With every new observation, the filter propagates the mean and the covariance of a system state to provide a new estimate. Therefore, the Kalman filter is suitable for the real time processing of data.[24] The system state is usually expressed as:

$$E_k = F_{k-1} E_{k-1} + w_{k-1}$$

while the observed system is given by:

$$y_k = H_k E_k + v_k$$

The random processes w_k and v_k are the system and the observation noises, respectively, which are assumed to be independent of each other with covariance matrices Q_k and R_k. F is a matrix that relates the previous to the current estimates, while the H matrix defines the relation between the measurement and the desired estimate. In the linear model of the drug release, F_{k-1} is constant and it is equal to $e^{-k_e \Delta t}$ while H_k is equal to 1.

Based on the system and measurements models, the filter is supposed to estimate the true encapsulation rate. A posteriori estimate E^+ of the state can be found if all the measurements up to the kth time are available. On the other hand, if all the measurements up to time $k-1$ are available, a priori E^- estimate of the state value at time k is found. In addition, Kalman filters provide a measure of the uncertainty in the state estimate at each iteration which is calculated by the estimation error covariance P. The filter algorithms can be summarized using the following equations:[28]

$$\begin{aligned}
E_k^- &= e^{-k_e \Delta t} E_{k-1}^+ + B_d, \\
P_k^- &= e^{-2k_e \Delta t} P_{k-1}^+ + Q, \\
K_k &= P_k^- (P_k^- + R)^{-1}, \\
P_k^+ &= (1 - K_k) P_k^-, \\
E_k^+ &= E_k^- + K_k (y_k - E_k^-)
\end{aligned}$$

4.2. Extended Kalman Filter

As stated previously, a non-linear model is used to capture the dynamics of this drug delivery system with its two segments, drug release and drug re-encapsulation. We propose the use of Extended Kalman Filters (EKF) to estimate the encapsulation rate E for this non-linear model. The EKF exploits the framework of Kalman filters to estimate the encapsulation rate at each iteration.[29] Series expansion and linearization techniques are employed by EKF to handle the non-linear dynamics of the state, expressed as

$$E_k = f(k-1, E_{k-1}) + w_{k-1}$$

and the measurement equation is given by

$$y_k = h(kE_k) + v_k$$

Both $f(\cdot)$ and $h(\cdot)$ are non-linear functions. The EKF follows the same structure as the Kalman filter except that it has one more linearization step. For each iteration the EKF carries an evaluation of the Jacobians, $F(k-1)$ and $H(k)$, using the following:

$$F(k-1) = \left.\frac{\partial f(k-1)}{\partial E}\right|_{E=E_{k-1}^+},$$

$$H(k) = \left.\frac{\partial h(k)}{\partial E}\right|_{E=E_k^-}$$

In the model, in $E(k) = \alpha(E(k-1))^2 + \beta E(k-1) + \gamma + w(k-1$, $f(\cdot)$ is a quadratic function of the state E whereas $h(\cdot)$ is a constant equal to 1. Hence, linearization is needed for the state equation only.

Using $(k-1) = \partial f(k-1)/\partial E|_{E=E_{k-1}^{+}}$, the state Jacobean $F(k-1)$ is calculated as:

$$F(k-1) = 2\alpha(E(k-1)) + \beta$$

It is important to note that the performance of EKF is dependent on the non-linearity of the model. If the model is highly non-linear, the linearization will poorly approximate the Jacobians which causes EKF to be a non-optimal solution.[29]

4.3. Particle Filter

A particle filter is also proposed to estimate the drug encapsulation. This Bayesian estimator is more flexible compared to the two other filters, it imposes no restriction on the system dynamics. Hence, particle filters can be used for both the linear and non-linear models. The key idea of this filter is to recursively calculate the required posterior probability $p(E \mid Y^k)$ using "importance sampling" and discrete random samples (particles). The particles used by the filter are associated with weights that are used to estimate the desired state.[30] In this section a detailed derivation of particle filter is provided.

Let $\{E_{0:k}^i, w_k^i\}_{i=1}^{N_s}$ be a set N_s particles $\{E_{0:k}^i, i = 1, \ldots, N_s\}$ associated with weights $\{w_k^i, i = 1, \ldots, N_s\}$ for encapsulation states E up to time k. The posterior PDF at time k can be then approximated by the following equation

$$p(E_{0:k} \mid y_{1:k}) \approx \sum_{i=1}^{N_s} w_k^i \delta(E_{0:k} - E_{0:k}^i)$$

The above equation is true under one constraint which is $\sum_{i=1}^{N_s} w_k^i = 1$.[25] Using the dirac delta function, a discretized approximation of the density is achieved. This approximation simplifies the computation of the desired density as it replaces all integrals by summations.[30] The next step is to choose the values of the w_k^i in what is called importance sampling. Now assume that the desired PDF $p(E)$ from which direct sampling is not possible. Moreover, assume another PDF $q(E)$ from which samples are generated, this PDF is known as the importance density.[25] Therefore, the approximation density can be given by

$$p(E) \approx \sum_{i=1}^{N_s} w^i \delta(E - E^i)$$

where the normalized weights are given by

$$w^i \propto \frac{p(E^i)}{q(E^i)}$$

The above equation can be expanded for all $E_{0:k}^i$

$$w_k^i \propto \frac{p(E_{0:k}^i)}{q(E_{0:k}^i)}$$

Using posterior representation, the weights can be given by

$$w_k^i \propto \frac{p(E_{0:k}^i \mid y_{1:k})}{q(E_{0:k}^i \mid y_{1:k})}$$

The posterior density equals to:

$$p(E_{0:k} \mid y_{1:k}) = \frac{p(y_k \mid E_{0:k}, y_{1:k-1}) p(E_{0:k} \mid y_{1:k-1})}{p(y_k \mid y_{1:k-1})}$$

Since the posterior density is recursively estimated, then all states up to time $k-1$ are available.

Hence, $p(E_{0:k} \mid y_{1:k-1})$ equals to:

$$p(E_{0:k} \mid y_{1:k-1}) = p(E_k \mid E_{0:k-1}, y_{1:k-1}) p(E_{0:k-1} \mid y_{1:k-1})$$

The posterior density then becomes:

$$p(E_{0:k} \mid y_{1:k}) = \frac{p(y_k \mid E_{0:k}, y_{1:k-1}) p(E_k \mid E_{0:k-1}, y_{1:k-1}) p(E_{0:k-1} \mid y_{1:k-1})}{p(y_k \mid y_{1:k-1})}$$

The above representation can be simplified to

$$= \frac{p(y_k \mid E_k) p(E_k \mid E_{k-1}) p(E_{0:k-1} \mid y_{1:k-1})}{p(y_k \mid y_{1:k-1})}$$

where $p(y_k \mid y_{1:k-1})$ is always true. Following from there, the posterior density becomes:

$$p(E_{0:k} \mid y_{1:k}) \propto p(y_k \mid E_k) p(E_k \mid E_{k-1}) p(E_{0:k-1} \mid y_{1:k-1})$$

Then we substitute the above equation in $w_k^i \propto p(E_{0:k}^i \mid y_{1:k})/q(E_{0:k}^i \mid y_{1:k})$ to obtain the updated weights:

$$w_k^i \propto \frac{p(y_k \mid E_k^i) p(E_k^i \mid E_{k-1}^i) p(E_{0:k-1}^i \mid y_{1:k-1})}{q(E_{0:k}^i \mid y_{1:k})}$$

Since the importance density can also be written in terms of previous states, the updated weights become:

$$w_k^i \propto \frac{p(y_k \mid E_k^i) p(E_k^i \mid E_{k-1}^i) p(E_{0:k-1}^i \mid y_{1:k-1})}{q(E_k^i \mid E_{0:k-1}^i, y_{1:k}) q(E_{0:k-1}^i \mid y_{1:k-1})}$$

The above can be simplified to:

$$\propto w_{k-1}^i \frac{p(y_k \mid E_k^i) p(E_k^i \mid E_{k-1}^i)}{q(E_k^i \mid E_{0:k-1}^i, y_{1:k})}$$

To further simplify the above equation, we can assume that the importance density is only dependent on the previous samples E_{k-1} and the current observation y_k. Therefore, the update weight equation can be reduced to:

$$w_k^i \propto w_{k-1}^i \frac{p(y_k \mid E_k^i) p(E_k^i \mid E_{k-1}^i)}{q(E_k^i \mid E_{k-1}^i, y_k)}$$

To simplify the above equation even further, the importance sampling density function can be chosen to be:

$$q(E_k \mid E_{k-1}^i, y_k) = p(E_k \mid E_{k-1}^i)$$

Hence, the weight update equation can be simplified to:

$$w_k^i \propto w_{k-1}^i p(y_k \mid E_k^i)$$

ALGORITHM 1 (GENERAL PARTICLE FILTER ALGORITHM).

1. **for** $i = 1$ to N_s **do**
2. Using $q(E_k^i \mid E_{k-1}^i, y_k)$, draw particles
3. Assign the particles weights using Eq. (28)
4. **end for**
5. Sum all weights $S = \sum_{i=1}^{N_s} W_k^i$
6. **for** $i = 1$ to N_s **do**
7. Normalize weights using $w_k^i = w^i / S_k$
8. **end for**
9. Resample using Algorithm 2
10. Find estimate E_k.

With this, we complete the basic Particle Filter equations. However, the procedure above is not enough for a particle filter to work, this is due to a degeneracy problem. This problem arises because, after few iterations of the above algorithm, all but few particles will have significant weight.[31] This means that few particles only will be contributing to the approximation of the density while the rest particles are useless.[25] Therefore, a resampling step is needed to ensure that samples with small weights are eliminated and the large weights are distributed over new samples such that all particle weights are equal.[31] The resampling step is shown in Figure 2. As is shown in the figure, the randomly drawn particles are weighted using the likelihood density. In the resampling step, the original particles are distributed such that they are concentrated around points with significant weights.

ALGORITHM 2 (SYSTEMATIC RESAMPLING ALGORITHM).

1. Initialize a variable $q(1) = 0$
2. **for** $i = 2$ to N_s **do**
2. $q(i) = q(i-1) + w_k^i$
3. **end for**
4. Initialize another variable $u(1) = \text{rand}/N_s$
6. **for** $j = 1$ to N_s **do**
7. Initialize $i = 1$
8. $u(j) = u(1) + (j-1)/N_s$
9. **While** $u(j) > c(i)$ **do**
10. $i = i + 1$
11. **end While**
12. $E_k^j = E_k^i$
13. $w_k^j = 1/N_s$

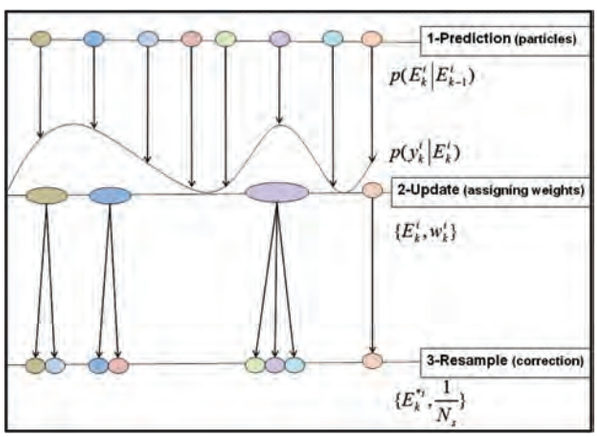

Figure 2. Illustration of the resampling step in particle filtering.

5. ADAPTIVE FILTERS

The high noise in the encapsulation measurement structure makes it hard to characterize the measurement noise covariance accurately, hence modeling errors are expected. Adaptive filters can be used to enhance the estimation performance of the filters for this case. An adaptive filter implements a multi-model filter approach that probabilistically determines the measurement noise covariance.[23] In the multi-model, several Kalman filters with different noise statistics assumptions will be used to estimate the state of encapsulation. The estimate of the state is found by probabilistically summing up the estimate from all filters in the model. The probability of each assumption is updated at each iteration by:

$$a_h(y(k)) = \frac{1}{\sqrt{2\pi R_h}} \exp^{\{-(1/2)y^T R_h y\}}$$

where R_h is the noise covariance assumption for the hth filter and $y(k)$ is the observation at time k. The probability that the assumption is correct given the measurements is also updated as:

$$A_h(k) = \frac{A_h(k-1) \times a_h(y(k))}{\sum_{h=1}^{n} A_h(k-1) \times a_h(y(k))}$$

From the above, the estimate state and covariance are found by:

$$E(k) = \sum_{h=1}^{n} A_h(k) \times E_h(k),$$

$$P(k) = \sum_{h=1}^{n} A_h(k) \times P_h(k)$$

A multi-model extended Kalman filter is implemented in this work for the non-linear model and particle filters are excluded from the multi-model analysis since they already embed an importance sampling technique in their algorithm.

6. EXPERIMENTAL RESULTS

In this section, we present the performance evaluation of Bayesian filters used to estimate the encapsulation rate for both true and simulated environments. Our experiments are implemented for the linear and nonlinear system dynamics. The simulated data are retrieved directly from the mathematical models while the real data are recorded from the customized experimental chamber. The real linear data are

obtained exclusively during sonication and the nonlinear data are recorded during and after sonication.

For comparisons in simulated environments, the models $E(k) = e - k_e \Delta t E(k-1) + Bd + w(k-1)$ and $y(k) = E(k) + v(k)$ are used to test the performance of Kalman filters, multi-model Kalman filters and particle filters. Then, extended Kalman filters, multi-model extended Kalman filters and particle filters are used to estimate the encapsulation rate for the nonlinear model (quadratic model) given by $E(k) = \alpha(E(k-1))^2 + \beta E(k-1) + \gamma + w(k-1)$ and $y(k) = E(k) + v(k)$. In both scenarios, the same system and measurement covariances are assumed for all filters, a system noise covariance of 0.5 and a measurement noise covariance of 0.02. For the multi-model adaptive filters, 5 measurement assumption covariances in the range of 0.06–0.02 were used with an initial 1/5 probability for each assumption.

Figure 3 shows the estimation results for the Kalman filter against the performance of the adaptive filter when used for predicting a linear system model in the simulated environment. Our results confirm previous findings[23] as is shown in the figure whereby the adaptive Kalman filter provides better results. Hence, the optimality of Kalman filters is achieved only when the correct modeling is guaranteed, which is achieved by using adaptive Kalman filters.

The performance of adaptive Kalman filter is then compared to the performance of the particle filter in a simulated environment. Particle filter performance is plotted against the adaptive Kalman filter in Figure 4. To achieve a good performance of the particle filter, 5000 particles are used to find the estimate which is computationally exhaustive. Although the particle filter performs reasonably well, the adaptive Kalman filter is optimal in this case since it is computationally less expensive.

The comparison between the adaptive Kalman filter and particle filter was extended to the real environment. Real data were used in Figure 5, where the adaptive Kalman and particle filter are used to predict drug encapsulation.

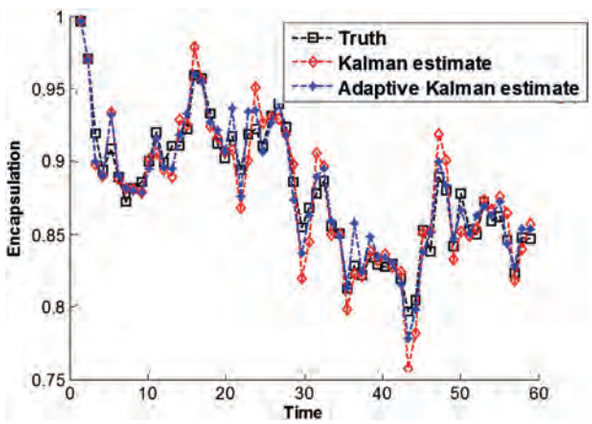

Figure 3. Simulated environment: The performance of adaptive Kalman versus Kalman filters.

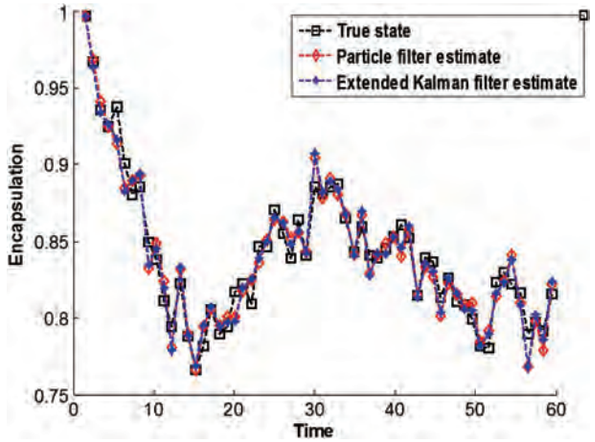

Figure 4. Simulated environment: The performance of adaptive Kalman versus particle filters.

The figure shows that, for real data, the adaptive Kalman filter is more stable than the particle filter. Therefore, adaptive Kalman filters outperform particle filters based on their computational requirements and stability.

The second part of our simulations is dedicated to the non-linear model (quadratic model) analysis. For this part of the study, extended Kalman filters were used for the non-linear model. In Figure 6, the performance of extended Kalman filter is plotted against the performance of adaptive extended Kalman filters. Both filters are used to estimate the non-linear states in a simulated environment. It is clear, from the results, that the adaptive filter outperforms the conventional extended Kalman filter.

Next, the particle filter is used to predict the encapsulation for the simulated data and its performance is compared to that of the adaptive extended Kalman filter. The results are shown in Figure 7. Similar to the linear model case, the good performance of the particle filter was only achieved after increasing the number of particles to 5000.

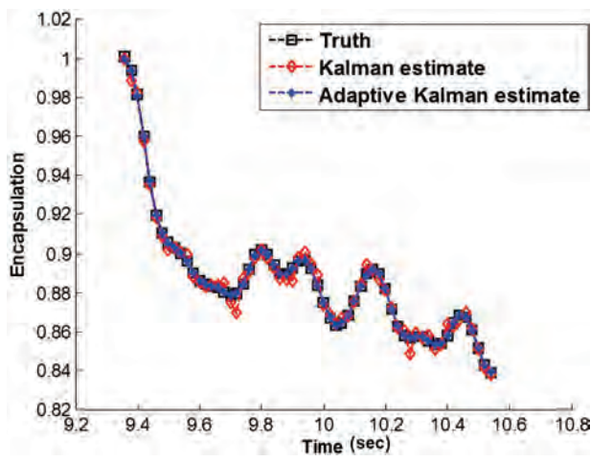

Figure 5. Real data: The performance of adaptive Kalman versus particle filters.

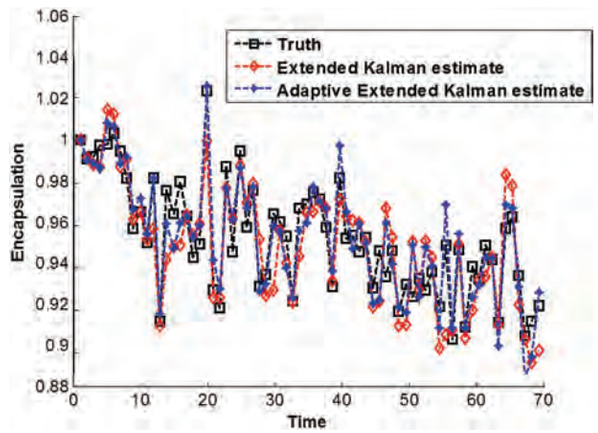

Figure 6. Simulated environment: The performance of adaptive extended Kalman versus extended Kalman filters.

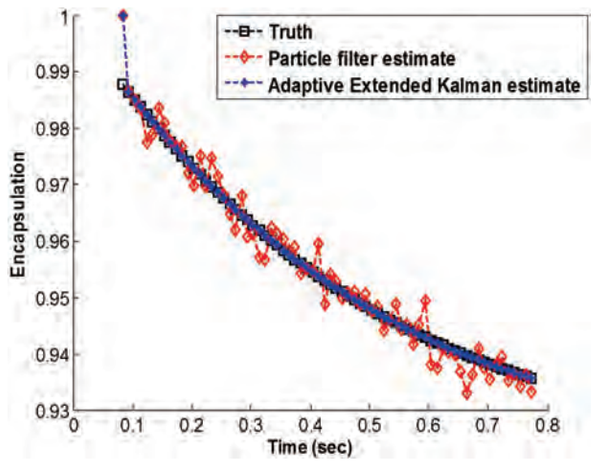

Figure 8. Real data: The performance of adaptive extended Kalman versus particle filters.

Although adaptive filters are known to outperform Kalman filters in predicting non-linear models, they are outperformed by Kalman filters for this specific model (representing drug release).

Finally, real non-linear experimental data are used, and the achieved estimation performances by the filters are depicted in Figure 8. With the real data, the adaptive extended Kalman filter is found to be more stable than the particle filter, indicating that for non-linear models extended Kalman filter is more stable and less computationally expensive than the particle filter.

It is worth mentioning that for the purpose of predicting drug release, the particle filter is advantageous for having the flexibility to predict both linear and non-linear models with the same code, unlike Kalman filters. However, the flexibility of particle filters comes at the expense of high computational complexity.

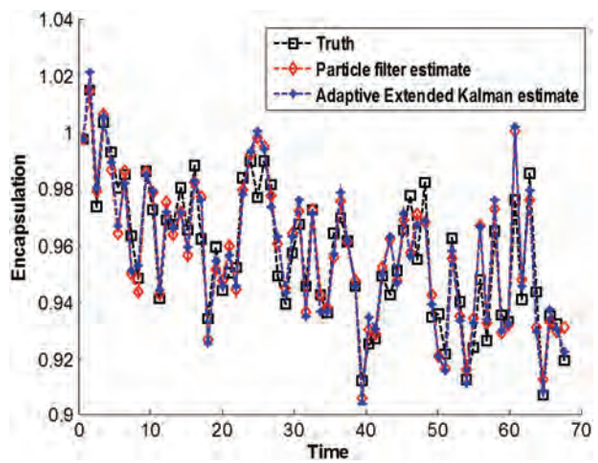

Figure 7. Simulated environment: The performance of adaptive extended Kalman versus particle filters.

7. CONCLUSIONS

This paper has discussed drug release estimation in an ultrasound-based drug delivery system. Two models of acoustically activated drug delivery systems were discussed and simulated; a linear and non-linear system models. The linear model describes the drug release process only whereas the non-linear model describes the whole drug delivery process. Several Bayesian filters were used to estimate the drug encapsulation rate. The filters performances were reported under real and simulated conditions. First, a Kalman filter and its adaptive (multi-model based) version were used to estimate the drug encapsulation rate. Our results show that the adaptive filter is more immune to modeling errors. The performance of the filters was checked when a linear model of the system was used. Using our results, we concluded that while a particle filter performed well, a Kalman filter is more stable and more computationally reliable. Additionally, the performance of the proposed filters was shown when a nonlinear model of the encapsulation was used. The results show that for the non-linear model an adaptive extended Kalman filter performs better than a normal extended Kalman filter. The adaptive extended Kalman filters, also, outperform particle filters. As part of our future work, the sensitivity and the consistency of the filters estimation performance will be studied.

Particle filters are very powerful Bayesian estimators that have no restrictions when it comes to the system and measurements dynamics. The objective of this paper was to study the possibility of replacing optimal Kalman filters with particle filters. The reason behind this objective is to eliminate the restrictions imposed by Kalman filters and provide a more flexible estimator (i.e., particle filter). Our results showed that a Kalman filter is indeed an optimal filter in linear and Gaussian problems. In addition, our results demonstrate that using a small number of particle Kalman filter performs better than particle filters.

The main goal of this drug delivery system is to reduce the side effects of conventional chemotherapy, hence improving the lives of cancer patients worldwide.

References and Notes

1. G. A. Husseini and W. G. Pitt, *Adv. Drug Deliv.* 60, 1137 (**2008**).
2. S. Ueno, J. Ando, H. Fujita, T. Sugawara, Y. Jimbo, K. Itaka, K. Kataoka, and T. Ushida, *IEEE Trans. Nanobiosci.* 5, 54 (**2006**).
3. D. Kanjickal and S. Lopina, *Crit. Rev. Ther. Drug Carrier Syst.* 21, 345 (**2004**).
4. Y. Bae and K. Kataoka, *Adv. Drug Deliv. Rev.* 61, 768 (**2009**).
5. J. Li, K. Caldwell, and N. Rapoport, *Langmuir* 10, 4475 (**1994**).
6. N. Rapoport and K. Caldwell, *Colloids Surf., B* 3, 217 (**1994**).
7. H. Gorcay, I. Celik, E. Yurdakul, Y. Sahin, and S. Kokten, *IEEE Sens. J.* 99, 1 (**2016**).
8. B. J. Staples, W. G. Pitt, B. L. Roeder, G. A. Husseini, D. Rajeev, and Schaalje, *J. Pharm. Sci.* 99, 31223131 (**2010**).
9. B. Staples, B. Roeder, G. Husseini, O. Badamjav, G. Schaalje, and W. Pitt, *Cancer Chemother. Pharmacol.* 64, 593 (**2009**).
10. Y. Ueno, S. Sonoda, R. Suzuki, M. Yokouchi, Y. Kawasoe, K. Tachibana, K. Maruyama, T. Sakamoto, and S. Komiya, *Cancer Biol. Ther.* 12, 270 (**2011**).
11. K. Tachibana, T. Uchida, K. Tamura, H. Eguchi, N. Yamashita, and K. Ogawa, *Cancer Lett.* 149, 189 (**2000**).
12. M. R. Prausnitz, S. Mitragotri, and R. Langer, *Nat. Rev. Drug Discov.* 3, 115 (**2004**).
13. N. Hijnen, S. Langereis, and H. Grll, *Adv. Drug Deliv. Rev.* 72, 65 (**2014**).
14. A. Partanen, P. S. Yarmolenko, A. Viitala, S. Appanaboyina, D. Haemmerich, A. Ranjan, G. Jacobs, D. Woods, J. Enholm, B. J. Wood, and M. R. Dreher, *Int. J. Hyperthermia* 28, 320 (**2012**).
15. Y. Qiu, C. Zhang, J. Tu, and D. Zhang, *J. Biomech.* 45, 1339 (**2012**).
16. G. A. Husseini, M. A. Diaz de la Rosa, E. S. Richardson, D. A. Christensen, and W. G. Pitt, *J. Control Release* 107, 253 (**2005**).
17. S. Rodamporn, N. Harris, S. Beeby, R. Boltryk, and T. Sanchez-Eisner, *IEEE Trans. Biomed. Eng.* 58, 927 (**2011**).
18. G. Husseini, L. Kherbeck, W. Pitt, J. Hubbell, D. Christensen, and D. Velluto, *J. Nanosci. Nanotechnol.* 15, 2099 (**2015**).
19. G. A. Husseini, M. A. D. de la Rosa, E. O. AlAqqad, S. A. Mamary, Y. Kadimati, A. A. Baik, and W. G. Pitt, *J. Franklin Inst.* 348, 125 (**2011**).
20. G. A. Husseini, N. M. Abdel-Jabbar, F. S. Mjalli, W. G. Pitt, and A. Al-Mousa, *J. Franklin Inst.* 348, 1276 (**2011**).
21. G. A. Husseini, M. A. D. de la Rosa, E. O. AlAqqad, S. A. Mamary, Y. Kadimati, A. A. Baik, and W. G. Pitt, *Technol. Cancer Res. Treat.* 8, 479 (**2009**).
22. G. Husseini, N. Abdel-Jabbar, F. Mjalli, and W. Pitt, *Technol. Cancer Res. Treat.* 6, 1 (**2007**).
23. M. Abdel-Hafez and G. Husseini, *IEEE Trans. Nanobiosci.* 14, 378 (**2015**).
24. S. Tatinati, K. C. Veluvolu, S. M. Hong, W. T. Latt, and W. T. Ang, *IEEE Sens. J.* 13, 4977 (**2013**).
25. M. S. Arulampalam, S. Maskell, and N. Gordon, *IEEE Trans. Signal Process.* 50, 174 (**2002**).
26. R. K. Tanbour, Using a cavitation model to represent the acoustic release kinetics from folated micelles, Master's thesis, American University of Sharjah (**2014**).
27. G. A. Husseini, D. Velluto, L. Kherbeck, W. G. Pitt, J. A. Hubbell, and D. A. Christensen, *Colloids Surf., B* 101, 153 (**2013**).
28. D. Simon, Optimal State Estimation: Kalman, H [Infinity] and Nonlinear Approaches, Wiley-Interscience, Hoboken, NJ (**2006**).
29. Y. Bar-Shalom, T. Kirubarajan, and X.-R. Li, Estimation with Applications to Tracking and Navigation, John Wiley & Sons, Inc., New York, NY, USA (**2002**).
30. P. M. Djuric, J. H. Kotecha, J. Zhang, Y. Huang, T. Ghirmai, M. F. Bugallo, and J. Miguez, *IEEE Signal Process. Mag.* 20, 19 (**2003**).
31. B. Ristic and Springer Link, Particle Filters for Random Set Models, Springer, New York, NY (**2013**).

Received: 17 July 2017. Accepted: 2 October 2017.